DOI: http://dx.doi.org/10.18524/1810-4215.2017.30.118314

IONISATION LOSS AND SHOCK EXCITATION OF $^{44}_{20}$Ca I AND $^{44}_{20}$Ca II ATOMS IN COLD REMNANTS OF TYPE II SUPERNOVAE

D.N.Doikov[1], S.M.Andrievsky[2,3]

[1] Odessa National Maritime University, Dep. of Mathematics, Physics and Astronomy, Odessa, Ukraine, *doikov@mail.bg*
[2] Astronomical Observatory, Odessa National University, and Isaac Newton Institute of Chile Odessa, Shevchenko Park, 65014 Odessa, Ukraine, *andrievskii@ukr.net*
[3] GEPI, Observatoire de Paris, PSL, Research University, CNRS, Univ. Paris Diderot, Sorbonne Paris Cite, Place Jules Janssen, 92195 Meudon, France

ABSTRACT. The light emission ("glow") of cold dusty plasma of the remnant of SN1987A was confirmed by the Hubble Space Telescope observations on 7th January, 1995. In particular, Ca I and Ca II lines were recorded and identified in the spectrum of the supernova's envelope. The period of complete hydrogen recombination in the remnant is 800 days. Thus, it is only radioactive decay that could be a primary source of the plasma light emission at the moment of observation. This paper describes the conditions of shock excitation and recombination of $^{44}_{20}$Ca resulted from the decay of radioactive $^{44}_{22}$Ti travelling in the remnant's cold dust. The over-ionisation in the remnant resulted from the motion of the $^{44}_{20}$Ca recoil nucleus, as well as its impact on the spectrum formation, was studied. It has been shown that the calcium lines are formed by the $^{44}_{20}$Ca II ion in the inner layers of the remnant. We have reached the conclusion that the Ca I/Ca II lines strength ratio corresponds to the isotopic abundance ratio $[^{40}_{20}\mathrm{Ca}]/[^{44}_{20}\mathrm{Ca}]$ in type II supernova remnants.

Keywords: SN1987A remnant, radioactive elements, spectroscopy of Ca I and Ca II.

1. Introduction

Calcium is an alpha-process element along with oxygen, neon, magnesium, silicon, sulphur, argon and titanium. The major source of calcium production in space is the synthesis in type II, Ib and Ic supernovae, as well as in exploding white dwarfs which are progenitors of type Ia supernovae. Large amounts of the stable isotope ^{40}Ca are synthesised in such processes. Its estimated abundance among other stable isotopes on Earth is about 97%. The stable isotope ^{44}Ca also makes a marked contribution, but its origin differs from the mechanism of synthesis of the most common isotope on the Earth. Exploding supernovae enrich the interstellar gas with various chemical elements, including calcium. Subsequently, the interstellar medium provides the raw material for the formation of new generation stars. Yellow supergiants with high luminosity, hence visible at long distances from the Sun, are the most relevant to studying the distribution of calcium in the Galactic disc. Cepheids are also among these objects. The lines of neutral and ionised calcium can be identified in the visible, near-ultraviolet and near-infrared portions of their spectra. As the ionised calcium lines in the near-ultraviolet spectral region are very strong, they cannot be used to determine the calcium abundance in the afore-mentioned stars. An example of calcium distribution in the Galactic disc inferred from the quantitative analysis of the spectra of a large number of Cepheids is presented in Fig. 1.

Cepheids are relatively young objects, hence their average calcium abundance at the galactocentric distance, which is close to the distance of the Sun from the Galactic centre (about 8 kiloparsecs), slightly exceeds the calcium abundance in the solar atmosphere.

As mentioned above, the ionised calcium lines in the near-ultraviolet spectral region cannot be used to precisely determine the calcium abundances in the atmospheres of stars with chemical compositions which do not differ much from that one of the solar atmosphere. However, the situation changes dramatically when we determine the chemical composition of extremely low-metallicity stars. Such stars can be found, for instance, in the halo of our Galaxy. With declining total metal content in a star its calcium abundance also decreases. It results in weakening of subordinate lines which generally serve as indicators of the calcium abundance in stars with normal metallicity. Thus, for extremely low-metallicity stars it is only feasible to use the ionised calcium lines in the near-ultraviolet spectral region (which are sufficiently weak in the spectra of such objects).

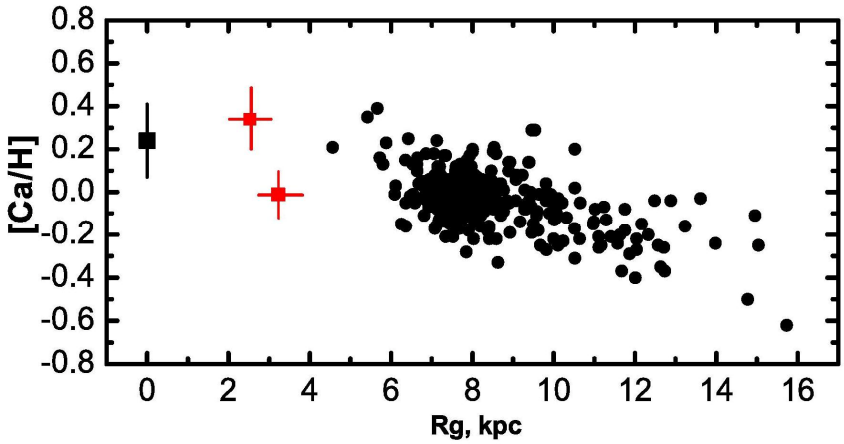

Figure 1: The radial distribution of calcium abundance in the Galactic disc inferred from the analysed spectra of Cepheids (marked with circles and two red squares based on the data reported in Andrievsky et al., 2014). The calcium abundance in the centre of the disc was adopted from the literature. The positions of two Cepheids which are the closest to the Galactic centre are marked with squares. The Y-axis shows [Ca/H] = log (Ca/H)$_*$ – log (Ca/H)$_{Sun}$ where the first term is attributed to the star while the second one – to the Sun; log (Ca/H) is the logarithm of the ratio of calcium to hydrogen concentration in the object's atmosphere. The X-axis presents Rg which is the distance from the Galactic centre expressed in kiloparsecs.

Table 1: The abundances of Ti, Sc and Ca isotopes (as reported by Popov et al., 2014; Jerkstrand et al., 2011) at the instant of ejection of the SN1987A envelope, as well as their estimated amounts at the present time expressed in solar masses.

Studies	$^{47}_{22}$Ti	$^{46}_{22}$Ti	$^{44}_{22}$Ti	$^{43}_{21}$Sc	$^{44}_{20}$Ca	$^{42}_{20}$Ca	$^{40}_{20}$Ca
Popov et al. (2014)	$5.25 \cdot 10^{-4}$	$4.86 \cdot 10^{-5}$	$1.73 \cdot 10^{-3}$	$5.75 \cdot 10^{-5}$	$5.91 \cdot 10^{-4}$	$5.91 \cdot 10^{-5}$	$6.23 \cdot 10^{-2}$
Jerkstrand et al. (2011)		$8.6 \cdot 10^{-4}$	$1.5 \cdot 10^{-3}$	$1.2 \cdot 10^{-6}$			0.043
Present study			10^{-3}		$1.0 \cdot 10^{-3}$		

2. Calcium atoms in the supernova remnant

The ionized calcium lines can be observed not only in the stellar spectra, but also in the ejecta spectra. The type II supernova remnants cool down noticeably while they expand. The formation of dust grains starts just under a year after the explosion. According to Kozasa et al. (1988), the formation of the dust component is only possible in the presence of condensation nuclei which are diatomic molecules. The rates of gas-phase reactions and nucleation decline significantly with time due to a drastic reduction in the material density. Within several decades, the particle density in the supernova remnants makes 10^4–10^6 cm^{-3}. The average thermodynamic temperatures of the ejecta, measured by the intrinsic infrared emission of the dust particles, are within the range of 30–70 K. When the blast wave moves rapidly away from the remnant, the intensity of hard radiation from the forward shock gradually decreases. For the remnants of SN1987A and Cas A, the International Gamma-Ray Astrophysics Laboratory (INTEGRAL) observations enabled us to reveal the evidence of radioactive decay of the titanium isotope which undergoes a two-phase series of β-process according to the following scheme:

$^{44}_{22}$Ti → $^{44}_{21}$Sc through the capture of a K-shell electron 1s ($p + e^- \rightarrow n + \nu_e$); the half-life of $^{44}_{22}$Ti is 48 years;

$^{44}_{21}Sc^* \rightarrow {}^{44}_{20}$Ca with emission of γ-quanta (67.9, 7, 4 and 1157 keV), positron e^+ and with transfer of a considerable momentum to the $^{44}_{20}$Ca nucleus; the half-life of the excited $^{44}_{21}Sc^*$ nucleus is 6 hours.

The decay phase described in item 1 is finished once the $^{44}_{21}$Sc nucleus has been formed. At the instant of time when the $^{44}_{21}$Sc nucleus is formed, it emits an electron neutrino. The nucleus gains a little recoil momentum (2–4 eV). The second phase of the radioactive decay, described in item 2, results in the transfer of high recoil kinetic energy of about 0.61–1.14 MeV to the $^{44}_{20}$Ca nucleus which acquires the velocity of around 10^5–10^6 m/s. When colliding with electrons and atoms of the cold supernova remnant, this energy is sufficient for either collisional ionisation or transition to an excited state. It is known that the total mass of the supernova remnant is M=19$M_\odot$, and its material density is $n \sim 10^{11} - 10^{12}$ m^{-3}. The change in the chemical composition of the supernova remnant envelope is an important effect of the processes specified in items 1 and 2. The initial isotopic composition of SN1987A that we are interested in is adapted from Popov et al. (2014) and given in Table 1.

At the present time, the stable isotope $^{40}_{20}$Ca abundance in the ejecta is an order of magnitude higher than that one of the $^{44}_{20}$Ca isotope. The remnant has greatly cooled down due to its expansion. Atoms of the primordial calcium, which is more abundant, have low

thermal velocities. Taking into account the given estimates, the average number of collisions of the $^{44}_{20}Ca$ isotope with the atoms of the supernova remnant material per unit of time can be calculated:

$$< z \geq = < v > \sqrt{2}\pi\sigma^2 n \approx 10^6 \cdot 1.41 \cdot 3.14 \cdot 2.64 \cdot 10^{-20} 10^{12} \approx 0.16\ \mathrm{s}^{-1} \quad (1)$$

The time interval between binary collisions $t_{binary} = \frac{1}{<z\geq}$ under the given physical conditions is $t \approx 6$ s. It far exceeds the characteristic time of radiative transitions associated with the atomic excitation. Before another mutual collision with atoms and electrons of the surroundings, the Ca I atom and Ca II ion efficiently interact with the radiation field exclusively. In the next section of the paper, we will estimate the energy losses due to excitation and ionisation of cold gas in the supernova remnant caused by the Ca I atom and its ion Ca II.

2.1. Ionisation loss in the cold remnants of SN1987A and Cas A

It is known that cold regions of supernova remnants comprise free radioactive atoms, molecules and dust containing radioactive components. Ionisation loss in the cold remnant is one of the ways their radioactivity manifests itself. The Ca I atom and its ion Ca II may be the sources of ionisation in the above-discussed decay chain. Given the recoil nucleus kinetic energy of 0.6 MeV and a rough non-relativistic approximation of the Bethe-Bloch formula, we can use its exact expression:

$$-\left(\frac{dW}{dx}\right)_{ion} = \frac{4\pi z^2 e^4 n_e}{m_e v^2}\left\{ln\frac{2m_e v^2}{I} - \beta^2 - ln(1-\beta^2)\right\} \quad (2)$$

where n_e is the electron density in the remnant; z_e is the charge of the particle ($z = 20$ for the calcium atom); v is the particle's velocity; β is the relativistic component which equals $\frac{v}{c}$, in our case $\beta \sim 0.01$; $\left(\frac{dW}{dx}\right)_{ion}$ is specific ionisation loss per unit of distance; I is the characteristic full ionisation potential, $I = (13.6$ eV)$\cdot z = 13.6 \cdot 20$ eV $= 270$ eV. The concentration of calcium ions at the forward propagating shock is many orders of magnitude lower than their concentration in the supernova remnant. The $^{44}_{20}$Ca isotope concentration is directly related to the number of decayed $^{44}_{22}$Ti nuclei. Ionisation loss in the material can be expressed as the linear energy loss L:

$$L = \frac{2\pi e^4 z^2 M n_e}{E m_e} \ln\left(\frac{4Em_e}{MI(z)}\right) \approx 2\ eV/10\ \mathrm{km} \quad (3)$$

Given the dimensions of the envelope, it can be deduced that all kinetic energy of calcium atoms is lost in radiative-loss processes. Let us determine the range of l_0 wherein the radiative loss diminishes the initial energy by a factor of e:

$$l_0 = \frac{4.31 \cdot 10^{26}}{n_e Z^2 \ln(183/Z^{1/3})} \approx 4.31 \cdot 10^{13}\mathrm{cm} \quad (4)$$

Physical dimensions of the envelope – remnant of SN 1987A are sufficient to ensure that the $^{44}_{20}$Ca atom transfers almost all kinetic energy in the form of radiative loss to ionise atoms of the remnant material. The process of ionisation of surroundings by the $^{44}_{20}$Ca ion involves binary collisions. In between such collisions, this ion interacts with the radiation field, and when reaching the outer layers of the envelope, its recombination takes place. By the time of recombination (which involves the capture of surrounding "cold" electrons), the $^{44}_{20}$Ca ion velocity decreases significantly down to the thermal velocity value. At this instant, it mixes with other calcium isotopes. The kinetic energy of positrons is proportional to the recoil energy of the $^{44}_{20}$Ca nuclei. The total energy loss of positrons in the remnant makes 10^{36} erg/s. Upon reaching the critical velocity, a positron collides with a cold electron that results in their annihilation and formation of two γ-quanta. The interaction between γ-quanta and gas is rather weak, but these γ-quanta heat the remnant's dust particles to some extent.

2.2. Triple recombination of the $^{44}_{20}$Ca II ions in SNR 1987A

The recombination coefficient α of the $^{44}_{20}$Ca II ion at its concentration N_i with the density of electrons density N_e and neutral atoms N_a in the thin remnant's envelope can be expressed as follows:

$$\frac{dN_i}{dt} = -\alpha N_\varepsilon N_\iota + \beta N_r N_a \quad (5)$$

Here the value β defines the ionisation coefficient of neutral atoms and molecules. To make the capture of an electron by a positively charged ion possible, the kinetic energy of their collision should convert into the energy carried away by the photon. In this case, the recombination cross-section contains the factor $\left(\frac{e^2}{hc}\right)^2$. The most accurate formula (5) for determination of the triple shock-recombination coefficient was inferred in the study by Smirnov (1968) by adjusting the level population of a given atom in the k^{th} state. We assume that N_k and N_n are the densities of atoms in relevant states; N_e is the density of electron states; v is the velocity of electrons; σ_{nk} is the cross-section of the transition of an excited atom from the state n to the state k. The product of the values in angle parentheses is averaged using the Maxwellian distribution function. The value γ_{nk} is the probability of the photon emission per unit of time when a given atom transits from the state n to the state k.

$$\frac{dN_k}{dt} = \sum_n \langle N_e v_e \sigma_{nk}\rangle - N_k \sum_n \langle N_e v_e \sigma_{nk}\rangle + \sum_n \langle N_n \gamma_{nk}\rangle - N_k \sum_n \langle \gamma_{nk}\rangle \quad (6)$$

If the recombination time is noticeably longer that the time interval between collisions of electrons, $\frac{dN_k}{dt} = 0$. In this case, the recombination process can be deemed to be quasi-stationary. As reported in the study referred above, at rather low temperatures the level population can be written as a Boltzmann distribution function. In this case, $N_k \sim e^{-E_{k/kT}}$. If the density of electrons is equal to the density of atoms at low temperatures, then allowing for the collisions with hydrogen, these equations will deliver the estimated coefficient of the shock-radiative recombination $\alpha \sim 10^{-6} cm^3/s$ at

N_e~10^{12} and T~30 – 60 K. If the mean free path of the $^{44}_{20}$Ca II ion is about one metre or greater, then the ion will have sufficient time to recombine prior to the next collision. At low temperatures, the energy of the $^{44}_{20}$Ca II ion collisions with free electrons is consistent with the ionisation energy. The shock-recombination and photo-recombination processes ought to be considered separately as they are not correlated.

We assume that the electron binding energy is E_0. A travelling $^{44}_{20}$Ca II ion undergoes predominantly binary collisions with the atoms of H I, He I, C I, N I, O I, Sc I and Ti I, as well as with electrons. When transiting to the reference system related to the travelling Ca ion, we can deduce that the ion is quiescent while the aforedescribed atoms and electrons have similar velocity 10^8 cm/s. At the instant of collision of the $^{44}_{20}$Ca II ions with any of the above mentioned atoms, a diatomic quasi-molecule is formed. If the adiabatic approximation whereby the motion of nuclei is neglected is true for this molecule, then the following expression is fair: $\frac{\omega Z_1 Z_2}{\mu v^2} \ll 1$ where ω is the energy difference between the investigated states; μ is the reduced mass of the quasi-molecule; v is the relative velocity. In other words, the adiabaticity of collisions is postulated when the Coulomb interaction potential is far lower than the kinetic energy of the incident atom. When $^{44}_{20}$Ca II is travelling in the envelope, this condition is met unless the ion reaches dense outer regions. In such regions the triple recombination is the most likely as the concentrations of hydrogen and helium are orders of magnitude higher than in the region of localisation of iron peak elements.

2.3. Calcium recombination in binary collisions

Incident electrons play a pivotal role in the $^{44}_{20}$Ca II recombination processes. At the time of the shock electron-ion recombination in low-temperature and low-density plasma of the supernova remnant, an electron is in a highly excited state. Thus, the recombination coefficient is defined by the rates of inelastic radiative transitions from highly excited states to the ground state. Let us give the triple recombination coefficients for the atoms of the alkali metals at T = 250K. For the electron density N_e~$10^8$and particle density of 10^{13} cm^{-3} the correspondent's coefficient's is $\alpha \approx 7.8 \cdot 10^{-11}$ and $2.6 \cdot 10^{-6}$. For the low-density plasma, the Born cross-section of inelastic transition is $\sigma = \frac{4\pi e^2}{h^2 v^2}|d_z|^2 L$ where L is the Coulomb logarithm that is not correlated with the relative velocity; d_z is the dipole moment operator. The production formulae can be inferred from the partition function counting all the states:

$$\sigma = \frac{4\pi}{3}\left(\frac{e^2}{hv}\right)^2 L(r^2), \qquad \alpha = const\,\frac{e^4}{h^2}\left(\frac{m}{T}\right)^{1/2}\frac{e^4}{T^2}\frac{e^6 N_i}{T^2} \quad (7)$$

In the study by Smirnov (1968) the constant is 1/3.

Let us present semiempirical recombination coefficients α for the Ca I atom and its ion Ca II in the radiation field of the supernova remnant at temperatures within the range of 10–1000K:

$$\alpha(T) = 27.9\left(\frac{T}{100}\right)^{-0.647};\ \text{Ca I: } \alpha(T) = 5.58\left(\frac{T}{100}\right)^{-0.683}$$

and the rate of photoionization resulted from Melender (2007) is as follows: Ca I: $(3.4-4.3)\cdot 10^{-10}$; Ca II: $(1.3-2.6)\cdot 10^{-12} s^{-1}$. The spontaneous velocities of the allowed dipole transitions can be written as per Landini (1972) and Melender (2007):

$$A_{ij}^{E1} = 2.6774 \cdot 10^9 \left(E_i - E_J\right)^3 \frac{1}{g_i} S_{ij}^{E1}\ (s^{-1}) \quad (8)$$

2.4. Characteristic time of the recombination transitions

The time at which an electron reaches the level with the binding energy of order of ~ T is denoted by τ_b; the time of recombination is denoted by τ_c. The rates of transitions from the state n to the state k, free-bound and bound-free transitions are denoted by ω_{nk}, ω_{cb} and ω_{bc}, respectively. With a rather high density of the supernova remnant the principle of detailed balance is fairly reasonable as the first approximation. Then, the time of transitions can be expressed as the continuum τ_c:

$$\tau_c = \frac{1}{\omega_{b0}}\frac{g_c}{g_0} \approx \frac{1}{N_e<v\sigma>}\frac{T^3}{e^6 N_i},\ \ \alpha = \left(\frac{1}{\tau N_\varepsilon}\right) \quad (9)$$

An alternative formulation of the Born approximation may be a relevant expression which factors in the energy difference between the recombination transitions from the level with the principal quantum number n to the ground (zero) level with the quantum number 0. In atomic units, the mass of an electron is used as a unit of mass; hence, the energy difference between the excited q_n and ground q_0 levels can be written as follows:

$$q_0 - q_n = \sqrt{2E_0} - \sqrt{2E_n} \approx \frac{2\Delta E}{\sqrt{E_0}} \quad (10)$$

where E_0 and E_n represent the electron energy before and after collision; ΔE is the atom's excitation energy. The following formula can be an additional validity criterion for the Born approximation: $\frac{a\Delta E}{\sqrt{E_0}} \ll 1$. Usage of this criterion significantly simplifies further calculations of the recombination process involving the $^{44}_{20}Ca$ II ion.

Using adiabaticity as a criterion, Bethe deduced a formula for recombination cross-section per one ionised atom (Haykawa, 1969):

$$\sigma_{on} = \frac{8\pi}{v_0^2}(D_x)_{0n}^2 Ln\frac{v'}{|v_0 - v_n|},\ \ D = \sum_i r_i \quad (11)$$

where D is the dipole moment operator; v_0 and v_n are the velocities of the incident electron before and after collision, respectively; v' is the average effective velocity in the region of invalidity of the Born approximation. The $^{44}_{20}$Ca II ion recombination coefficient can be estimated using observations of the structure of the supernova remnant's envelope and localization of the main fraction of the radioactive titanium isotope $^{44}_{22}$Ti performed during Hubble observations of SNR1987A on 7th January, 1995, can be used. In most models of the supernova remnant, the radioactive titanium is concentrated in the same region as iron. The average number density of the iron atoms N_{Fe} at the time of observations was 10^4 cm^{-3}. The electron density N_e is about 0.14 N_{Fe}.

In the same region, 60% of the total $^{44}_{22}$Ti and other heavy elements are found. The mixing ratio between the layers is insignificant; hence, the abundance of $^{44}_{22}Ti$ in other layers is lower. In outer layers containing H and He atoms, the respective density reaches 10^{12} –10^{13} particles per cm^3. At the same time, titanium is absent in these layers while $^{44}_{20}$Ca II penetrating these layers recombines into a neutral $^{44}_{20}$Ca I atom.

2.5. Formation of the remnant spectrum in the ultraviolet (UV), optical and near-infrared (NIR) regions

The Hubble Space Telescope observations of SNR 1987A were conducted in the spectral region from 200 to 800 nm. The observations proved that the escaping radiation spectrum corresponds to the thermodynamic temperature which is 300 K higher than reported by the observations of the dust emission in the infrared region. The formation of the UV and optical radiation fluxes of sufficient intensity requires highly efficient conversion of the radioactive decay energy into the thermal energy of the envelope. In other words, γ-quanta, positrons and recoil nuclei should be thermalized. Taking into account that at present the level of radioactive decays remains practically unaltered while the density and abundance decreased t^3 times, the current abundance is two-three orders of magnitude lower than observed in 1995.

However, γ-quanta and X-rays easily escape from the remnant thereby slightly heating the dust. Thus, positrons with energy of about 0.6 MeV and $^{44}_{20}$Ca recoil nuclei with the kinetic energy of the same order are expected to be the key contributors to the energy balance of the envelope. The subsequent excitation of atoms and molecules occurs via three channels:

The first channel is induced by the UV and other shortwave quanta of the radiation field and results in the formation of the lines of Mg I, Mg II (282.5 nm), Fe II (373 nm), O II (372.7 nm), Ca II((397.3 nm, 730.63 nm).

The second channel is related to the ionization loss due to positron and $^{44}_{20}$Ca recoil nucleus deceleration. The fluxes of energy formed by these shock excitation sources throughout the remnant make up about $4{\cdot}10^{36}$erg/s. The total volume of the envelope at the moment of observations was $V = 10^{50}$ cm^3 (or 30 erg s^{-1}cm^{-3}). The probability of electron transitions from the excited levels to the adjacent levels is significantly higher than the likelihood of recombination transitions. Thus, within the range of radiative losses L_0, the $^{44}_{20}$Ca atom will be in the ionised state while the density of atoms and free electrons in the envelope will decline. It means that calcium is more likely to be in the ionised state rather than in the neutral state as far as the end of the decelerating path. When the kinetic energy of the atom becomes comparable to the particle thermal-motion energy, the recombination of the ion into the neutral Ca atom occurs. In this case, the methods for calculation of the detailed balance for quantum bound states can be employed. The optical and infrared transitions of the neutral atoms of the supernova remnant were analysed in accordance with the data reported by Jerkstand et al. (2011). One of the ways to independently determine the mass fraction of calcium produced by the decay chain is to estimate the ionised and neutral Ca line strengths and their ratios.

The third channel is associated with the cascade transitions caused by the high rate of excitation of $^{44}_{20}$Ca atoms, as well as target atoms in the initial phase of the recoil nucleus motion. These transitions are displayed mainly in the hard UV region, and after conversion by the iron atoms they form an observed field of the remnant radiation in the optical and infrared regions of the spectrum.

The non-thermal source of energy supply resulting from the radioactive decays in the supernova remnant produces excessive scattered non-thermal radiation which is not typical for the diffusion radiation in nebulae. On the other hand, the supernova remnant is quantitatively characterized by the same physical parameters as the nebulae. The absence of the central compact source of hard quanta is offset by the inner radioactive transformations. This effect leads to collisions, induces ionization loss in the remnant and forms a radiation field of sufficient intensity. The Ca II/ Ca I line strength ratio is an important indicator of the radioactive decay processes in the investigated physical system "cold gas + radioactive isotopes". However, this question requires in-depth investigation and should be the focus of a separate paper.

3. On the possibility of the presence of calcium molecular compounds in the supernova cold envelope

Most of diatomic molecules are formed within one year after the explosion. Compounds with rather high ionisation potential are of special interest as the shortwave radiation does not destroy, but only excite the molecules. Both absorption and emission lines are formed: the former belong to the optical and near-infrared regions while the latter represent emission in the far infrared and radio regions. Another condition for the existence of diatomic molecule is the presence of inhomogeneous clumps caused by the Rayleigh-Taylor instability when the material falls on the iron nucleus. Later, these clumps isolate themselves and exhibit densities which are several orders of magnitude higher than the density of the surrounding gas. The probability of the formation of dust and molecules in these clumps is higher. One year later, the dust particles accounting for these clumps efficiently absorb hard UV and X-ray radiation. This enables the dust to screen molecules from quanta which cause their dissociation. The envelope inhomogeneities, which had already isolated within 10–12 years after the explosion, were studied by Varosi & Dwek (1999). Statistical distribution of these inhomogeneities by the data size made it possible to estimate their average size using a sample of one thousand recorded data units. The clumps themselves gradually expand due to their excessive internal pressure. Enhancing the sensitivity of instruments, as well as allowing for the geometric factor, results in the increased number of recorded clumps. Observations of old remnants of type II supernovae confirm these conclusions.

Table 2: The spectroscopic molecular constants for CaO (in cm^{-1})

State	T_{00} – Term energy	State weight (g_i)	Internuclear distance (A)	B_e	α_ε	ω_e	$\omega_e x_e$
$X^1\Sigma$	0.0	1	1.822	0.44452	0.00338	733.4	5.28
$A^1\Pi$	8225	2	2.097	0.3353	0.0015	556.2	2.30

The cellular structure in the envelope should be further considered with the application of the formalism suggested by Varosi & Dwek (1999). We suggest that the spherical approximation should be solved first to determine the lines of elements best suitable for the physical and observational analyses, and then the problem should be solved using a relevant Monte-Carlo method to allow for the specific cellular structure of the object observed.

4. Isotopic composition of the SN1987A envelope

The strengths of molecular lines in the supernova remnant and at the forward shock have greatly increased recently while the X-ray and infrared radiation fluxes have declined. Apart from the suggested criterion for the selection of isotopes by the Ca II and Ca I atomic line strength ratio, let us consider the possibility of the determination of the isotopic shift in the molecules involving $^{44}_{20}$Ca , $^{42}_{20}$Ca and $^{40}_{20}$Ca isotopes while the isotopic ratio gradually changes due to the radioactive $^{44}_{22}$Ti decay.

The isotopic shift in the diatomic molecules depends on the atomic mass numbers. As reported in Herzberg (1949), such a correlation can be expressed as a function of molecular constants of compounds in the parent molecule containing, for instance, $^{40}_{20}$Ca, and the ratio given by the following formula:

$$\rho = \sqrt{\mu_{^{44}_{20}\mathrm{Ca}} \Big/ \mu_{^{40}_{20}\mathrm{Ca}}} = \sqrt{44/40} \approx 1.05.$$

From all diatomic molecules involving calcium isotopes formed in the envelope we select molecules with the maximum ionisation potential and the highest sensitivity to the isotopic shift ρ. The selected molecules should have the highest density and population of the excited levels both at present and in the future. Molecules selected in such a manner ought to exhibit well-measured absorption lines in the UV, visible and NIR regions of the remnant's spectrum. Among diatomic molecules containing Ca atoms in the stellar spectra, the CaO molecule is the most stable with the dissociation potential D_0 = 5–6.11 eV. According to the survey results and new findings reported in Pavlenko & Schmidt (2015), the dissociation energy of the CaH molecule is 1.686–1.974 eV. The detection of the CaC molecule is expected though its ionisation coefficient is an order of magnitude lower than that one of CaH. Thus, the calcium oxide (CaO) molecule appears to be most suitable for the determination of the isotopic shift of spectral lines. The ratios reported in Jorgensen (1994) and Herzcberg (1949) can be applied to perform an assessment of the isotopic shift. It is reasonably convenient to conduct such an analysis for the band heads reported in Doikov et al. (2017) for the transition $A^1\Pi \rightarrow X^1\Sigma$ using the molecular constants given in Table 2 below. The vibrational band-head shift in this case is 4.9183021 cm^{-1} or 4.1 Å in the near-infrared region. In the optical band, this shift will be an order of magnitude less and within the accuracy of spectrometric measurements.

5. Conclusion

The present paper shows the feasibility of observing and identifying the lines of neutral and singly ionised calcium. The availability of the lines of this element for the observations and its involvement in the radioactive decay chain $^{44}_{22}\mathrm{Ti} \xrightarrow{85\,y} {}^{44}_{21}\mathrm{Sc} \xrightarrow{6\,h} {}^{44}_{20}\mathrm{Ca}$ enables us to use the calcium isotope as a chemical marker of the evolution processes in the ejecta of supernova remnants. Different molecular lines appear in the remnant's spectrum after 20–30 years after the supernova explosion. In this regard, the CaO molecule is of special interest. We suppose that the ^{44}Ca/^{40}Ca isotopic abundance ratio may be inferred from the CaO molecular lines using high-resolution spectroscopy.

References

Andrievsky, S.M., Martin, K. P., Kovtuykh, V.V. et al.: 2016, *MNRAS*, **461**, 4256.

Doikov D.N., Savchuk N.V., Yushchenko A.V.: 2017, Odessa Astron. Publ., **30**, 69.

Landini M., Monsignori B.C., Fossi: 1972. *A&A*, **7**, 291.

Melender M., Bautista M.A., Badnell N.R.: 2007, *A&A*, **469**, 1208.

Kozasa T., Yasegava H. and Nomoto K.: 1989, *ApJ*, **344**, 325.

Jerkstand A., Fransson C. and Kozma C.: 2011, *A&A*, **530**, A45, 1-23.

Jorgensen U.G.: 1994, *A&A*, **284**, 179.

Hayakawa S.: 1969, Cosmic ray physics. Nuclear and astrophysics aspects. J. Wiley & Sons. N.Y.

Herzberg G.: 1949, Spectra and Molecular Structure. Van Norst. Reinhold, N.Y.

P'equignot D. and Aldovandi S.M.: 1986, *A&A*, **161**, 169.

Popov M.V., Filina A.A. et al.: 2014, *ApJ*, **783**, 43(Spp).

Pavlenko Ya.V., Schmidt M.: 2015, *Kinem. and Phys. of Cel. Bod.*, **31**, issue 2, 90.

Smirnov B.M.: 1968, Atomic collision and elementary processes in plasma, Moscow: Atomizdat.

Varosi F. & Dwek E.: 1999, *ApJ*, **523**, 265.